A&A 440, 751–758 (2005)
DOI: 10.1051/0004-6361:20042376

Astronomy & Astrophysics

The CORALIE survey for southern extra-solar planets

XIII. A pair of planets around HD 202206 or a circumbinary planet?

A. C. M. Correia[1,2,3], S. Udry[1], M. Mayor[1], J. Laskar[3], D. Naef[4], F. Pepe[1], D. Queloz[1], and N. C. Santos[1,5]

[1] Observatoire de Genève, 51 Ch. des Maillettes, 1290 Sauverny, Switzerland
e-mail: acorreia@fis.ua.pt
[2] Departamento de Física da Universidade de Aveiro, Campus Universitário de Santiago, 3810-193 Aveiro, Portugal
[3] Astronomie et Systèmes Dynamiques, IMCCE-CNRS UMR 8028, 77 avenue Denfert-Rochereau, 75014 Paris, France
[4] European Southern Observatory, Casilla 19001, Santiago 19, Chile
[5] Centro de Astronomia e Astrofísica da Universidade de Lisboa, Tapada da Ajuda, 1349-018 Lisboa, Portugal

Received 17 November 2004 / Accepted 12 May 2005

Abstract. Long-term precise Doppler measurements with the CORALIE spectrograph reveal the presence of a second planet orbiting the solar-type star HD 202206. The radial-velocity combined fit yields companion masses of $m_2 \sin i = 17.4\ M_{\rm Jup}$ and $2.44\ M_{\rm Jup}$, semi-major axes of $a = 0.83$ AU and 2.55 AU, and eccentricities of $e = 0.43$ and 0.27, respectively. A dynamical analysis of the system further shows a 5/1 mean motion resonance between the two planets. This system is of particular interest since the inner planet is within the brown-dwarf limits while the outer one is much less massive. Therefore, either the inner planet formed simultaneously in the protoplanetary disk as a *superplanet*, or the outer *Jupiter-like* planet formed in a circumbinary disk. We believe this singular planetary system will provide important constraints on planetary formation and migration scenarios.

Key words. techniques: radial velocities – techniques: spectroscopic – stars: individual: HD 202206 – stars: binaries: general – stars: planetary systems

1. Introduction

For about 6 years, the CORALIE planet-search programme in the southern hemisphere (Udry et al. 2000) has been ongoing on the 1.2 m Euler Swiss telescope, designed, built and operated by the Geneva Observatory at La Silla Observatory (ESO, Chile). During this time, the CORALIE radial-velocity measurements have allowed us to detect close to 40 extra-solar planets. Interestingly, brown-dwarfs candidates, easier to detect with high-precision Doppler surveys, seem to be more sparse than exoplanets (Mayor et al. 1997), especially in the 10–40 $M_{\rm Jup}$ interval (Halbwachs et al. 2000), the so called *brown-dwarf desert*. Objects in this domain are very important to understand the brown-dwarf/planet transition. The distinction between planets and brown dwarfs may rely on different considerations such as mass, physics of the interior, formation mechanism, etc. From the "formation" point of view, the brown-dwarf companions belong to the low-mass end of the secondaries formed in binary stars while planets form in the protostellar disk. Such distinct origins of planetary and multiple-star systems are clearly emphasized by the two peaks in the observed distribution of minimum masses of secondaries to solar-type stars (e.g. Udry et al. 2002). They strongly suggest different formation and evolution histories for the two populations: below 10 $M_{\rm Jup}$ the planetary distribution increases with decreasing mass and is thus not the tail of the stellar binary distribution.

In this context, the 17.5 $M_{\rm Jup}$ minimum mass companion detected around HD 202206 (Udry et al. 2002, Paper I) provided an interesting massive planet or low-mass brown-dwarf candidate. Contrary to HD 110833 which was detected with a comparable $m_2 \sin i$ companion (Mayor et al. 1997) and then was shown to be a stellar binary (Halbwachs et al. 2000), the distance of HD 202206 (46.3 pc) prevents the HIPPARCOS astrometric data from constraining the visual orbit. At such a distance the expected minimum displacement on the sky of the star due to the inner companion is only 0.26 mas, largely insufficient for the HIPPARCOS precision. If not due to unfavorable orbital inclination, the observed low secondary mass sets the companion close to the limit of the planetary and brown-dwarf domains.

Apart from the massive planet candidate, the radial-velocity measurements of HD 202206 also revealed an additional drift with a slope of $\sim$43 ms^{-1} yr^{-1} pointing towards the presence of another companion in the system (Paper I). The long-term follow-up of HD 202206 is now unveiling the nature of the second companion: a planet about ten times less massive than

the inner one. If we assume that the outer planet was formed in the stellar protoplanetary disk, the inner planet likely also formed there, and therefore is not a brown dwarf. This means that protoplanetary disks may be much more massive than usually thought. Inversely, if we assume that the inner body was formed as a brown dwarf, then either the outer planet was also formed as a brown dwarf, or it was formed in an accretion disk around the binary composed of the main star and the brown dwarf.

Dynamically, the present system is also very interesting. The large mass of the inner planet provokes high perturbations in the orbit of the outer one. The system is thus in a very chaotic region, but the existence of a 5/1 mean motion resonance in this region allows it to stabilize the orbits of the planets in this system.

The stellar properties of HD 202206 are briefly recalled in Sect. 2, The radial velocities and the new detected companion are described in Sect. 3. The stability of the system is examined in Sect. 4 and the possible implications of such a system on the planet versus brown-dwarf formation paradigm are discussed further in Sect. 5.

2. HD 202206 stellar characteristics

The HD 202206 star was observed by the HIPPARCOS astrometric satellite (HIP 104903). A high-precision spectroscopic study of this star was also performed by Santos et al. (2001) in order to examine the metallicity distribution of stars hosting planets. Observed and inferred stellar parameters from these different sources are summarized in Table 1, taken from Paper I.

The high metallicity of HD 202206 probably accounts for its over luminosity ($M_V = 4.75$, ~0.4 mag brighter than the expected value for a typical G6 dwarf of solar metallicity) as $T_{\rm eff}$ is also larger than the value expected for a G6 dwarf.

The dispersion of the HIPPARCOS photometric data of HD 202206 ($\sigma_{\rm Hp} = 0.013$ mag) is slightly high for the star magnitude but some indication of stellar activity is seen in the spectra.

The radial-velocity jitter associated with intrinsic stellar activity of rotating solar-type stars may have induced spurious radial-velocity noise, decreasing our ability to detect planetary low-amplitude radial-velocity variations. Although noticeable, the activity level of HD 202206 is not very large (Paper I, Fig. 2). It adds only some low-level high-frequency spurious noise in the radial-velocity measurements, taking into account the small projected rotational velocity of the star and the long period of the newly detected planet.

3. Orbital solutions for the HD 202206 system

The CORALIE observations of HD 202206 started in August 1999. The obvious variation of the radial velocities allowed us to announce the detection of a low-mass companion of the star after one orbital period. When a second maximum of the radial-velocity curve was reached, we noticed a slight drift of its value. With 95 measurements covering more than 3 orbital periods, a simultaneous fit of a Keplerian model and a linear drift yielded a period of 256 days, an eccentricity $e = 0.43$ and a secondary minimum mass of 17.5 $M_{\rm Jup}$ (Paper I). The slope of the radial-velocity drift was found to be 42.9 $\rm ms^{-1}\ yr^{-1}$, and the available measurements did not allow us to further constrain the longer-period companion.

Table 1. Observed and inferred stellar parameters for HD 202206. Photometric, spectral type and astrometric parameters are from HIPPARCOS (ESA 1997). The atmospheric parameters $T_{\rm eff}$, log g, [Fe/H] are from Santos et al. (2001). The bolometric correction is computed from Flower (1996) using the spectroscopic $T_{\rm eff}$ determination. The given age is derived from the Geneva evolutionary models (Schaerer et al. 1993) which also provide the mass estimate.

Parameter		HD 202206
Spectral Type		G6V
V		8.08
$B-V$		0.714
π	[mas]	21.58 ± 1.14
M_V		4.75
BC		−0.082
L	[$L_\odot$]	1.07
[Fe/H]		0.37 ± 0.07
M	[$M_\odot$]	1.15
$T_{\rm eff}$	[K]	5765 ± 40
log g	[cgs]	4.75 ± 0.20
$v \sin i$	[km s^{-1}]	2.5
age	[Gyr]	5.6 ± 1.2

After 105 CORALIE radial-velocity measurements we are now able to describe the orbit of the third body in the system. Surprisingly, the former observed drift was not the result of a stellar companion, but the trace of a not very massive planet in a 1400 day orbit with eccentricity $e = 0.27$. Indeed, the outer planet minimum mass of 2.44 $M_{\rm Jup}$ is almost ten times less massive than the inner one.

Using the iterative Levenberg-Marquardt method (Press et al. 1992), we first attempt to fit the complete set of radial velocities from CORALIE with a single orbiting companion and a linear drift as we did in Paper I (solution **S1**). This fit implies a companion with $P = 255.9$ days, $e = 0.43$ and a minimum mass of 17.7 $M_{\rm Jup}$ (Table 2), similar to our previous values (Paper I). However, the slope of the radial velocity drift now drops to 4.96 $\rm ms^{-1}\ yr^{-1}$, indicating that something changed after the consideration of the additional data. Such is also inadequate, as the velocity residuals exhibit rms = 23.45 $\rm ms^{-1}$, while the measurement uncertainties are only ~8 $\rm ms^{-1}$. In particular, this fit gives a reduced $\sqrt{\chi^2} = 3.66$, clearly casting doubt on the model. Using a quadratic drift instead of a linear one (solution **S2**), we get identical values for the companion orbital parameters (Table 2), and slightly improve our fit, obtaining $\sqrt{\chi^2} = 2.52$ (Fig. 1).

3.1. Two independent Keplerian fits

Here we try to fit the radial velocities with two orbiting planetary companions moving in two elliptical orbits without interaction (solution **S3**). The orbits can thus be described by

Table 2. Orbital parameters of a single companion orbiting HD 202206 including drifts in the fit. We consider two cases: a linear drift (**S1**) and a quadratic drift (**S2**). This last model improves the fitted solution, but is still unsatisfactory as we also add one more degree of freedom. λ is the mean longitude of the date ($\lambda = \omega + M$) and errors are given by the standard deviation σ.

Param.	S1 & S2	linear (S1)	quadratic (S2)
rms	[m/s]	23.45	15.62
$\sqrt{\chi^2}$		3.66	2.52
Date	[JD–2 400 000]	52 250.00 (fixed)	52 250.00 (fixed)
V	[km s^{-1}]	14.730 ± 0.001	14.752 ± 0.001
P	[days]	255.86 ± 0.03	256.04 ± 0.03
λ	[deg]	263.51 ± 0.10	265.04 ± 0.12
e		0.431 ± 0.001	0.440 ± 0.001
ω	[deg]	157.61 ± 0.27	159.75 ± 0.28
K	[m/s]	573.26 ± 1.17	566.75 ± 1.22
T	[JD–2 400 000]	52 174.7 ± 0.2	52 175.1 ± 0.2
$k_l\ t$	[m/s/yr]	4.96 ± 0.49	10.69 ± 0.55
$k_q\ t^2$	[m/s/yr^2]	–	−17.29 ± 0.66
$a_1 \sin i$	[10^{-3} AU]	12.17	11.98
$f(m)$	[$10^{-9}\ M_\odot$]	3669	3497
$m_2 \sin i$	[$M_{\rm Jup}$]	17.7	17.5
a	[AU]	0.83	0.83

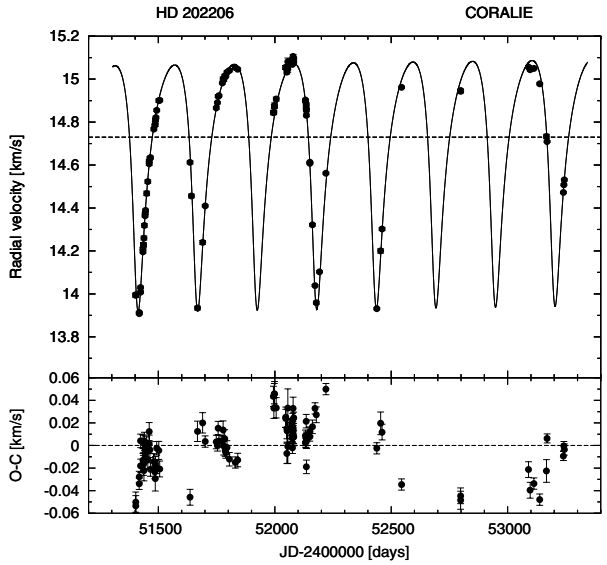

Fig. 1. CORALIE radial velocities for HD 202206 with a single planet and a linear drift (**S1**). We see that many points lie outside the fitted curve and the value of the reduced $\sqrt{\chi^2} = 3.66$ is unacceptable.

two independent Keplerians as separate two-body problems, without accounting for mutual planetary perturbations.

The two-planet Keplerian fit to the radial velocities using the Levenberg-Marquardt method yields for the inner planet $P = 256.2$ days, $e = 0.43$ and a minimum mass of 17.5 $M_{\rm Jup}$, while for the new companion $P = 1297$ days, $e = 0.28$ and a minimum mass of 2.41 $M_{\rm Jup}$ (Table 3). The velocity residuals in this two-planet model drops to rms = 9.81 ms^{-1} and the reduced $\sqrt{\chi^2}$ is now 1.53, clearly suggesting that the

Table 3. Orbital parameters of two planets orbiting HD 202206 using a two independent Keplerian model (**S3**). We neglect the gravitational interactions between the two planets, but we obtain a better fit than using a single planet with a drift (Table 2). Errors are given by the standard deviation σ.

Param.	S3	inner	outer
rms	[m/s]	9.81	
$\sqrt{\chi^2}$		1.53	
Date	[JD–2 400 000]	52 250.00 (fixed)	
V	[km s^{-1}]	14.721 ± 0.001	
P	[days]	256.20 ± 0.03	1296.8 ± 19.1
λ	[deg]	265.60 ± 0.13	31.54 ± 2.67
e		0.433 ± 0.001	0.284 ± 0.046
ω	[deg]	161.10 ± 0.31	101.83 ± 6.60
K	[m/s]	564.83 ± 1.45	42.71 ± 2.00
T	[JD–2 400 000]	52 175.6 ± 0.2	51 206.4 ± 29.9
$a_1 \sin i$	[10^{-3} AU]	11.99	4.88
$f(m)$	[$10^{-9}\ M_\odot$]	3502	9.22
$m_2 \sin i$	[$M_{\rm Jup}$]	17.5	2.41
a	[AU]	0.83	2.44

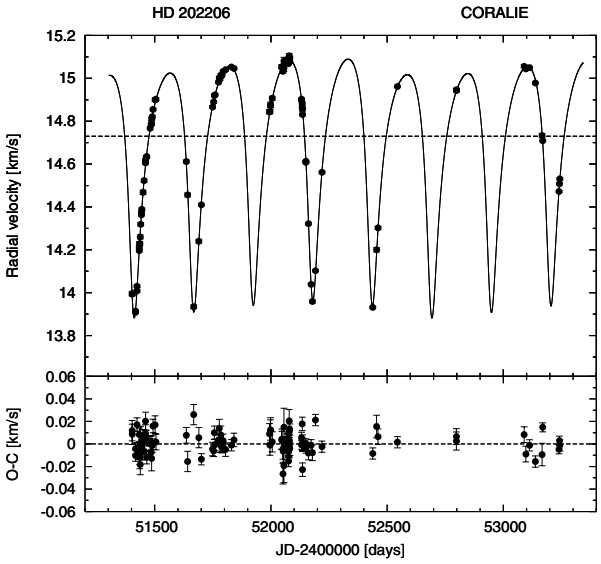

Fig. 2. CORALIE radial velocities for HD 202206 with a two independent Keplerian model (**S3**). The residuals are smaller than in the case obtained with only one planet (Fig. 1) and the value of the reduced $\sqrt{\chi^2} = 1.53$ is also better.

two companion model represents a significant improvement, even accounting for the introduction of four additional free parameters. The Levenberg-Marquardt minimization method rapidly converges into local minima of the χ^2. However, there is no guarantee that this minimum is global. Thus, we also fitted our data using a genetic algorithm starting with arbitrary sets of initial conditions. The found orbital parameters are identical to the Levenberg-Marquardt solutions. We hence conclude that our χ^2 value is the best for the present data.

The necessity of the second planet is demonstrated visually when we compare Figs. 1 and 2 showing CORALIE

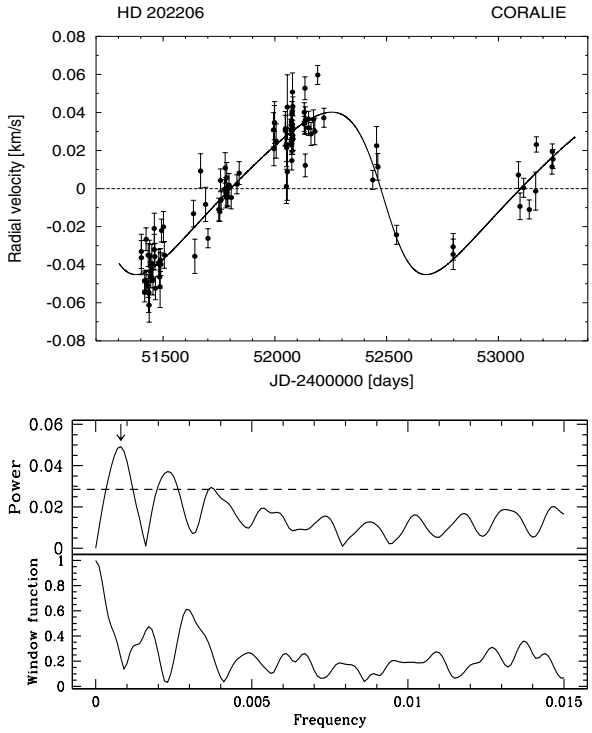

Fig. 3. CORALIE residual radial velocities for HD 202206 when the contributions from the inner planet are subtracted (*top*) and respective frequency analysis and periodogram. The data acquired before JD = 2 452 200 showed a linear trend that could be provoked by a distant binary companion. However, the data acquired after that date clearly shows a short period companion. The dotted line in the power spectra shows the height of the largest aleatory peak obtained after 100 000 random Monte Carlo simulations. This corresponds to a false alarm probability of less than 10^{-5}.

radial velocities and the associated residuals. In Fig. 3 we plotted the orbit of the second planet in the radial velocity residuals of the inner planet. We also show the frequency analysis of this data and a respective periodogram of the velocity residuals. The largest frequency peak ($\approx$0.0007 day^{-1}) corresponds to the period of the outer planet and there are no aliases. Finally, we computed false alarm probabilities for the second planet through Monte Carlo simulations by randomly shuffling the data. The dotted line in the power spectra of the inner planet residuals (Fig. 3) shows the height of the largest aleatory peak obtained after 100 000 random simulations. The amplitude of this peak is 0.023 m/s, that is, about one half of the amplitude of the main peak of the second planet spectra ($\approx$0.045 m/s). This gives a false alarm probability of less than 10^{-5}.

3.2. Planet-planet interaction

Due to the proximity of the two planets and to their high minimum masses (in particular to the inner planet's huge mass), the gravitational interactions between these two bodies will be quite strong. This prompt us to fit the observational data using a 3-body model (solution **S4**), similarly to what has been done for the system GJ 876 (Laughlin & Chambers 2001; Laughlin et al. 2004). Assuming co-planar motion perpendicular to the plane of the sky, we get slightly better results for $\sqrt{\chi^2}$ and velocity residuals (Table 4) than we got for the two-Keplerian fit. The improvement in our fit is not significant, but there is a striking difference: the 3-body fitted orbital parameters of the outer planet show important deviations from the two-Keplerian case. We then conclude that, although we still cannot detect the planet-planet interaction in the present data, we will soon be able to do so. We have been following the HD 202206 system for about five years and we expect to see this gravitational interaction in less than another five years. Thus, two complete orbital revolutions of the outer planet around the star should be enough. In Fig. 4 we plot the two fitting models evolving in time and we clearly see detectable deviations between the two cruves appearing in a near future.

Finally, we also fitted the data with a 3-body model where the inclination of the orbital planes was free to vary (as well as the node of the outer planet). We were unable to improve our fit, even though we have increased the number of free parameters by three. Therefore, the inclination of the planets remains unknown, as do their real masses.

Table 4. Orbital parameters of two planets orbiting HD 202206 using 3-body model (**S4**). We take into account the gravitational interactions between the two planets, but we obtain a similar fit to the two-Keplerian model (Table 3). However, the orbital parameters of the outer planet are different. Errors are given by the standard deviation σ.

Param.	S4	inner	outer
rms	[m/s]	9.65	
$\sqrt{\chi^2}$		1.47	
Date	[JD–2 400 000]	52 250.00 (fixed)	
V	[km s^{-1}]	14.721 ± 0.001	
P	[days]	255.87 ± 0.06	1383.4 ± 18.4
λ	[deg]	266.23 ± 0.18	30.59 ± 2.84
e		0.435 ± 0.001	0.267 ± 0.021
ω	[deg]	161.18 ± 0.30	78.99 ± 6.65
K	[m/s]	564.75 ± 1.34	42.01 ± 1.50
i	[deg]	90.00 (fixed)	90.00 (fixed)
$a_1 \sin i$	[10^{-3} AU]	11.96	5.15
$f(m)$	[10^{-9} $M_\odot$]	3487	9.51
$m_2 \sin i$	[$M_{\rm Jup}$]	17.4	2.44
a	[AU]	0.83	2.55

4. Orbital stability

In this section we briefly analyze the dynamical stability of the orbital parameters obtained in the previous section. A more detailed study of the system behavior will be presented in a forthcoming paper.

4.1. Dynamical evolution

In last section we saw that there were two different models to fit the observational data: a simplified model using independent Keplerian orbits for each planet (**S3**) and a 3-body dynamical model (**S4**). Tracking the dynamical evolution of both sets of

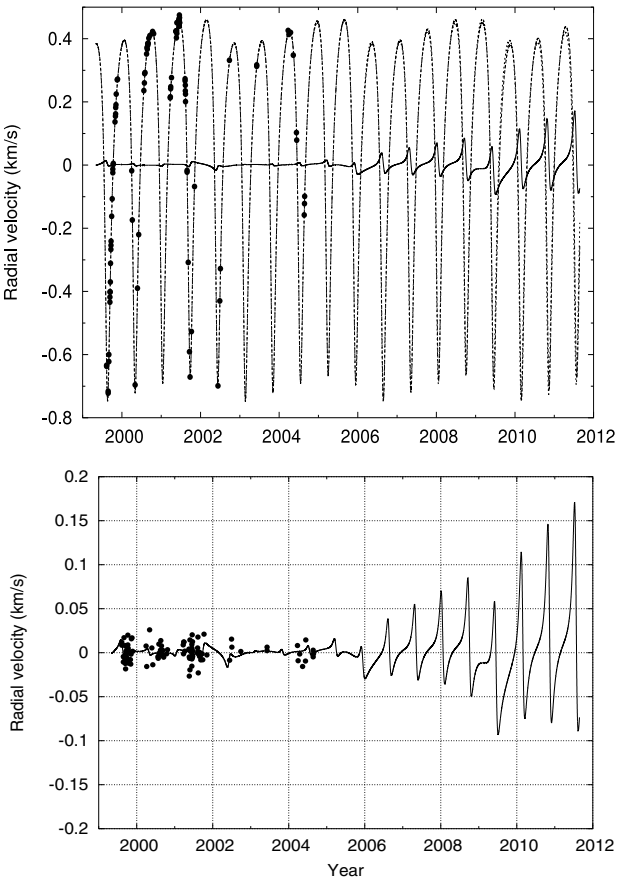

Fig. 4. Radial velocities differences between the two independent Keplerian model (Table 3) and the 3-body model (Table 4). Data coincides at JD = 2 452 250 (Dec. 6th 2001). In the bottom figure we plotted the velocity residuals of the two Keplerian fit. Since CORALIE's precision is about 8 m/s for this star, we expect to observe these differences in the coming years.

parameters in the future, we find that the two systems become unstable in a few thousand years (Fig. 5). For the initial parameters obtained with the orbital solution S3, the outer planet is lost after only five thousand years, the same happening with the system S4 at about forty thousand years. This last solution is a slightly better determination of the planetary system around HD 202206, although it is still very unsatisfactory. It can nevertheless be used as a starting point for a dynamical study of this system.

4.2. Stable solutions

Since the estimated age of the HD 202206 star is about 5 Gyr (Table 1), it is clear that the previous orbits are not good. One reason is that the fitted parameters still present some uncertainties around the best fitted value. This is particularly true for the outer planet, with a small semi-amplitude variation of about 40 m/s. Moreover, in order to fit our observational data to the theoretical radial-velocity curve, we used the iterative Levenberg-Marquardt method. This method converges to a minimum χ^2, but other close local minima may represent as well a good fit for our data. Additionally, there may exist other planets in the system that will also perturb the present solution. We should thus consider that the set of parameters given in Sect. 3 constitutes the best determination one can do so far, and we will search for more stable solutions in its vicinity.

Starting with the orbital solution S4, obtained with the 3-body model (Table 4), we have searched for possible nearby stable zones. Since the orbit of the inner planet is well established, with small standard errors, we have kept the parameters of this planet constant. We also did not change the inclination of the orbital planes, keeping both at 90°. For the outer planet we let a, λ, e and ω vary. Typically, as in Fig. 6 we have fixed e and λ to specific values, and have spanned the (a, ω) plane of initial conditions with a step size of 0.005 AU for a and 1 degree for ω. For each initial condition, the orbit of the planets are integrated over 2000 years with the symplectic integrator SABAC4 of Laskar & Robutel (2001), using a step size of 0.02 year. The stability of the orbit is then measured by frequency analysis (Laskar 1990, 1993). Practically, a refined determination of the mean motion n_2, n_2' of the outer planet is obtained over two consecutive time interval of length T = 1000 years, and the measure of the difference $D = \left|n_2 - n_2'\right| / T$ (in deg/yr^2 in Fig. 6) is a measure of the chaotic diffusion of the trajectory. It should be close to zero for a regular solution and high values will correspond to strong chaotic motion (see Laskar 1993 for more details).

In the present case a regular motion will require $D < 10^{-6}$. We find that the vicinity of the HD 202206 system is very chaotic (light grey region of Fig. 6) and the majority of the initial conditions will rapidly become unstable. Because of the two planets' proximity and large values of the masses and eccentricities, the chaotic behavior was expected. We nevertheless find a small region of initial conditions (the darker region of Fig. 6) with very small diffusion and where the trajectories remain stable for several million years. These orbital solutions correspond to the resonant island of an orbital 5/1 mean motion resonance.

Labeled lines of Fig. 6 give the value of $\sqrt{\chi^2}$ obtained for each choice of parameters. We observe that the minimum χ^2 obtained for the present data is effectively in a zone of high orbital diffusion. Stable orbits can only be found inside the dark spot, which corresponds to the 5/1 mean motion resonance. In order to find stable solutions coherent with our data, we need to increase χ^2 until we get initial conditions inside this resonant zone. Thus, the best fit that provides a stable orbital solution will present $\sqrt{\chi^2} \sim 1.7$, which is still acceptable. For instance, choosing $\omega = 55.50°$ and $a = 2.542$ AU (solution **S5**), we have $\sqrt{\chi^2} = 1.67$ (Table 5).

Henceforward, we will consider that the solution S5 (with orbital parameters given in Table 5) is more representative of the real behavior of the HD 202206 planetary system. Ideally, we would like that the best fit to the observation would also be in a stable region, but we assume that in the present case, this requirement is not satisfied because of the limited time span and resolution of the observations that do not allow us to solve precisely for the outer planet elements. In particular, we have not been able yet to solve for the mutual inclination of the planets that may also shift the location of the regular resonant island.

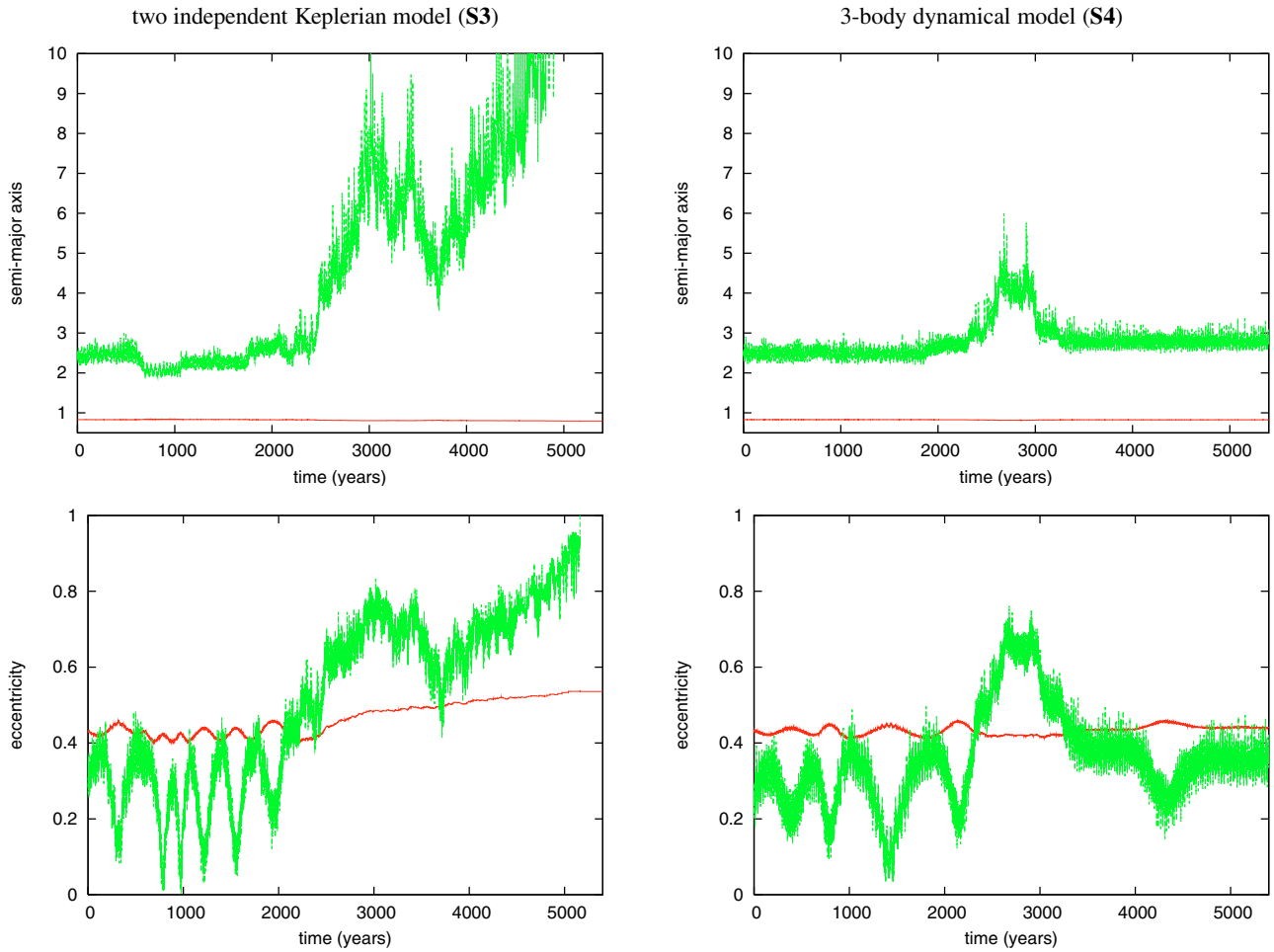

Fig. 5. Dynamical evolution of the semi-major axis and eccentricity for two different sets of initial parameters. On the left we plotted the evolution for S3 initial parameters obtained with a two independent Keplerian model (Table 3), while on the right we used the S4 initial parameters from the 3-body dynamical model (Table 4). Both sets of initial parameters are unstable, although S4 is a little better (the outer planet is only lost after forty thousand years).

Table 5. Stable orbital parameters for the two planets orbiting HD 202206. Using the orbital solution S4 (Table 4), we chose the values of the perihelium and the semi-major axis of the outer planet such that the system becomes stable. The new system is in a 5/1 mean motion resonance.

Param.	S5	inner	outer
a	[AU]	0.83040	**2.54200**
λ	[deg]	266.22864	30.58643
e		0.43492	0.26692
ω	[deg]	161.18256	**55.50000**
i	[deg]	90.00000	90.00000
m	[$M_{\rm Jup}$]	17.42774	2.43653
Date	[JD–2 400 000]	52250.00	
rms	[m/s]	**10.73**	
$\sqrt{\chi^2}$		**1.67**	

For the orbital solution S5, the main resonant argument is

$$\theta = \lambda_1 - 5\lambda_2 + g_1\, t + 3g_2\, t \quad (1)$$

where g_1 and g_2 are fundamental secular frequencies of the system related to the perihelion of the inner and outer planet respectively (see Laskar 1990). Both are retrograde, with periods $P_{g_1} \approx 399\,000$ yr and $P_{g_2} \approx 339$ yr. The resonant argument θ is in libration around $\theta_0 = 76.914$ deg, with a libration period $P_\theta \approx 19.4$ yr, and an amplitude of about 37 degrees (Fig. 7). It should be noted that for the real solution, the libration amplitude may be smaller, but the libration period will be of the same order of magnitude, that is around 20 years. The observation of the system over a few additional years may then provide an estimate of the libration amplitude and thus a strong constraint on the parameters of the system.

4.3. Secular evolution

Using the S5 stable orbital parameters (Table 5) we have first integrated our system over a few thousand years (Fig. 7). Unlike results plotted in Fig. 5 for unstable systems, we now observe a regular variation of the eccentricity of both planets.

Because of the strong gravitational interactions with the inner planet, the outer planet still shows large variations in its

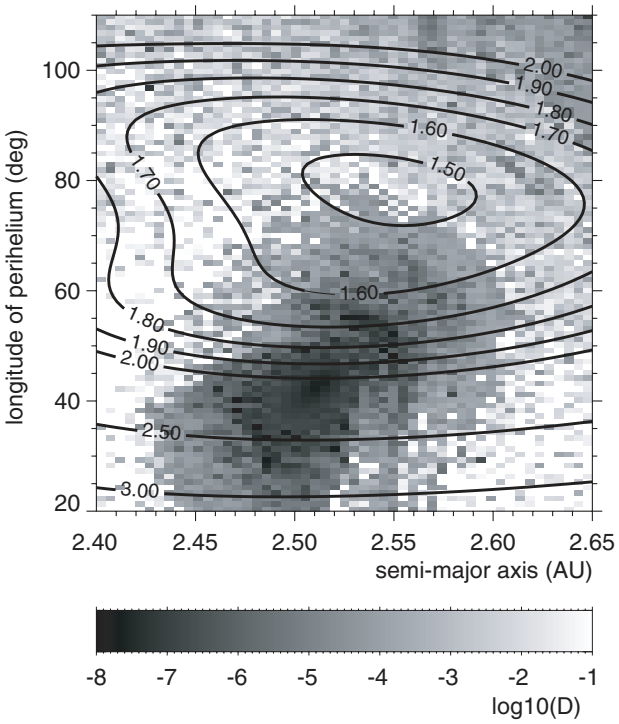

Fig. 6. Global view of the dynamics of the HD 202206 system for variations of the perihelium and semi-major axis of the outer planet. Light grey areas correspond to high orbital diffusion (instability) and dark areas to low diffusion (stable orbits). The grey scale is the stability index (D) obtained through a frequency analysis of the longitude of the outer planet over two consecutive time intervals of 1000 yr. Labeled lines give the value of $\sqrt{\chi^2}$ obtained for each choice of parameters. Initial conditions in the dark spot stable zone (with $\log_{10}(D) < -6$) are trapped in a 5/1 mean motion resonance.

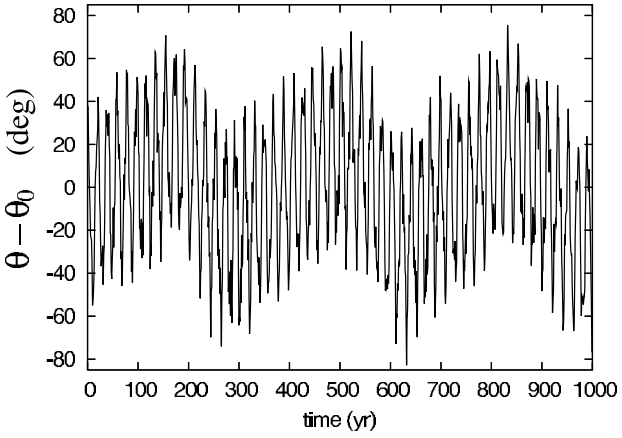

Fig. 7. In the orbital solution S5 (Table 5), the resonant argument $\theta = \lambda_1 - 5\lambda_2 + g_1\,t + 3g_2\,t$ is in libration around $\theta_0 = 76.914$ deg, with a libration period $P_\theta \approx 19.4$ yr, and an amplitude of about 37 degrees.

orbital parameters. The eccentricity can range from less than 0.1 to about 0.45, while the semi-major axis varies between 2.3 and almost 3 AU. As a result, the minimum distance between the two planets' orbits is only 0.4 AU. However, because of the 5/1 mean motion resonance trapping, the two planets never come closer than about 1.1 AU. We also observe rapid secular variations of the orbital parameters, mostly driven by

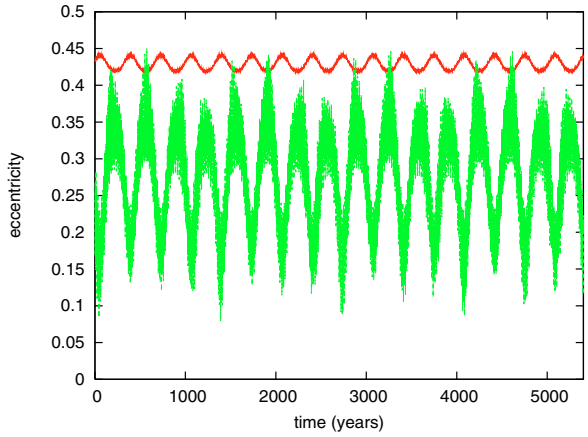

Fig. 8. Dynamical evolution of the eccentricity with the orbital solution S5 (Table 5). As expected, the eccentricity presents regular variations that contrasts to the irregular behavior of the orbital solutions presented in Fig. 5. Due to the strong gravitational interactions, the secular variations of the eccentricity are rapid, and mostly driven by the secular frequency g_2, with period $P_{g_2} \approx 339$ yr.

the rapid secular frequency g_2, with a period $P_{g_2} \approx 339$ yr. These secular variations of the orbital elements are much faster than in our Solar System, and should make possible their direct observation.

The S5 orbital parameters (determined using the global view of the system dynamics given by Fig. 6) allow us to obtain an orbital evolution of the system that is much more satisfactory than the one obtained by a direct orbital fit (Sect. 3, solutions S3 and S4), as the system now remains stable within five thousand years (Figs. 5 and 7). Although from the previous stability analysis (Sect. 4.2) we know that the stability of the orbit is granted for a much longer time interval than the few thousand years of the orbital integration, we have also directly tested the stability of the system S5 over 5 Gyr. The results displayed in Fig. 8 show that indeed, the orbital elements evolve in a regular way, and remain relatively stable over the age of the central star.

5. Discussion and conclusion

In this paper we report the presence of a second planet orbiting the HD 202206 star, whose orbital parameters are quite unexpected. This system was first described as a star orbited by a massive planet or a light brown dwarf (Udry et al. 2002, Paper I). The first CORALIE measurements already suggested the presence of a second, longer period companion, but it was thought to be a very distant stellar companion. The existence of a second, much less massive body at only 2.55 AU, was never observed and troubles our understanding of the hierarchy of planetary systems. Two other multiple planetary systems were discovered with orbital periods identical to this one: HD 12661 (264 and 1445 days) and HD 169830 (226 and 2102 days). However, the mass ratio of the two planets differ in both cases by less than a factor of two, while for HD 202206 this ratio is almost ten. Mazeh & Zucker (2003) suggested that a possible correlation between mass ratio and period ratio in multiple planetary systems may exist. Using the multiple

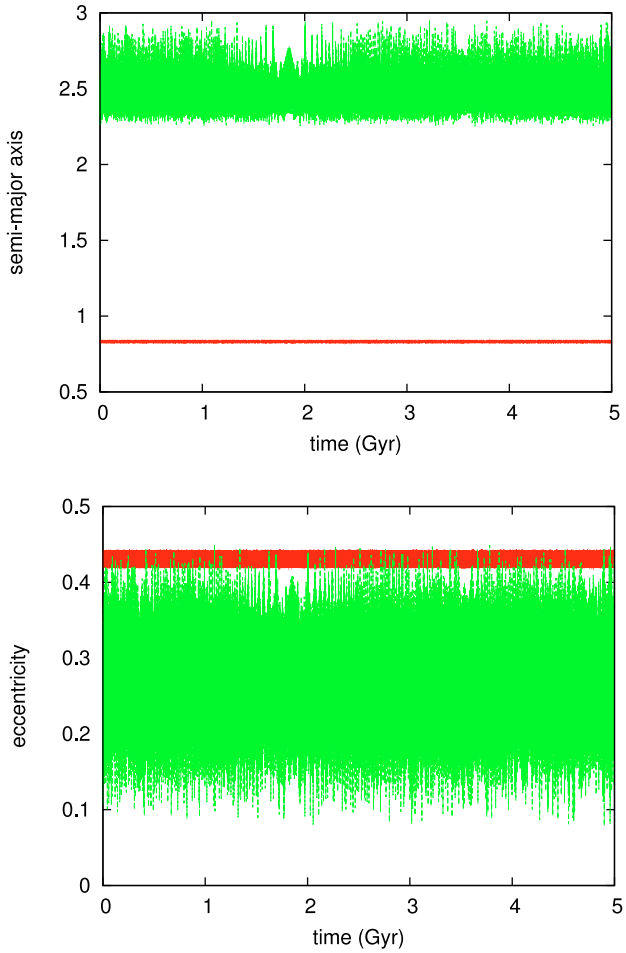

Fig. 9. Long term evolution of the semi-major axis and the eccentricity for both planets with the orbital solution S5 (Table 5). The system remained stable during 5 billion years. The small variation in the semi-major axis and eccentricity around 2 Gyr is probably due to some very slow diffusion through a small resonance.

planetary systems discovered to the date (including Jupiter and Saturn), they found that, except for the 2/1 resonant systems, the correlation between the logarithms of the two ratios was 0.9498. In order to keep this result, the consideration of the present planetary system shows that mean motion resonances other than the 2/1 should probably also be excluded from the correlated systems.

These observations raise the question of how this system was formed, bringing additional constraints to the existent theories. Supposing that the inner body is effectively a brown dwarf, then the new found planet will be an example of a planet in a binary, formed in the circumbinary protoplanetary disk. This assumption seems to be a real possibility, since recent numerical simulations show that a planet formed in a circumbinary disk can migrate inward until it is captured in resonance (Nelson 2003). Inversely, we can suppose that both companions were formed in the accretion disk of the star, with the result that the inner planet is not a brown dwarf. This leads to the re-definition of the brown-dwarf limits and requires that the initial disk around HD 202206 was much more massive than we would usually think.

Dynamically the system is very interesting and promising. The gravitational interactions between the two planets are strong, but stability is possible due to the presence of a 5/1 mean motion resonance with a libration period of about 20 years. This is the first observation of such an orbital configuration that may have been reached through the dissipative process of planet migration during the early stages of the system evolution.

The strong gravitational interactions among the planets may also allow us to correctly model their effect in the nearby future. With the current precision of CORALIE, fixed at about 8 m/s for HD 202206, we are presently close to detecting the trace of the planet-planet interactions in data. This will be reached even sooner with the higher precision measurements presently obtained with the ESO HARPS spectrograph at a ∼1 m/s level (Mayor et al. 2003). The planet-planet interaction signature may provide important information on the inclination of the orbital planes and allow us to determine the mass values of both planets.

Acknowledgements. We are grateful to the staff from the Geneva Observatory which maintains the 1.2-m Euler Swiss telescope and the CORALIE echelle spectrograph at La Silla. This work was supported by Geneva University, the Swiss NSF (FNRS) and from PNP-CNRS. A.C. also benefited from the support of the HPRN-CT-2002-00308 European training network programme.

References

ESA 1997, ESA-SP, 1200
Flower, P. J. 1996, ApJ, 469, 355
Halbwachs, J.-L., Arenou, F., Mayor, M., Udry, S., & Queloz, D. 2000, A&A, 355, 581
Laskar, J. 1990, Icarus, 88, 266
Laskar, J. 1993, Phys. D, 67, 257
Laskar, J., & Robutel, P. 2001, Celest. Mech., 80, 39
Laughlin, G., & Chambers, J. E. 2001, ApJ, 551, L109
Laughlin, G., Butler, R. P., Fischer, D. A., et al. 2004, ApJ, 622, 1182
Mayor, M., Queloz, D., Udry, S., & Halbwachs, J.-L. 1997, in Astronomical and Biochemical Origins and the Search for Life in the Universe, ed. R. Cosmovici, S. Browyer, & D. Werthimer, IAU Coll., 161, 313
Mayor, M., Pepe, F., Queloz, D., et al. 2003, The Messenger, 114, 20
Mazeh, T., & Zucker, S. 2003, ApJ, 590, L115
Nelson, R. P. 2003, MNRAS, 345, 233
Press, W. H., Teukolsky, S. A., & Flannery, B. P. 1992, Numerical Recipes: the art of scientific computing (Cambridge: Cambridge Univ. Press)
Schaerer, D., Charbonnel, C., Meynet, G., Maeder, A., & Schaller, G. 1993, A&A, 102, 339
Santos, N. C., Israelian, G., & Mayor, M. 2001, A&A, 373, 1019
Udry, S., Mayor, M., Naef, D., et al. 2000, A&A, 356, 590
Udry, S., Mayor, M., Naef, D., et al. 2002, A&A, 390, 267 (Paper I)